Case-based reasoning adaptation of numerical representations of human organs by interpolation

Julien Henriet(1), Pierre-Emmanuel Leni(1), Rémy Laurent(1), Michel Salomon(2)

(1) Université de Franche-Comté, Chrono-Environnement UMR 6249 CNRS
4 Place Tharradin, 25200 Montbéliard, France
(2) Université de Franche-Comté, FEMTO-ST UMR 6174 CNRS
Rue Engel Gros, 90000 Belfort, France
julien.henriet,pierre-emmanuel.leni,remy.laurent,michel.salomon@univ-fcomte.fr

Abstract

Case-Based Reasoning (CBR) and interpolation tools can provide solutions to unknown problems by adapting solutions from other problems already solved. We propose a generic approach using an interpolation tool during the CBR-adaptation phase. The application EquiVox, which attempts to design three dimensional representations of human organs according to external measurements, was modelled. It follows the CBR-cycle with its adaptation tool based on Artificial Neural Networks and its performances are evaluated and discussed. The results show that this adaptation tool meets the requirements of radiation protection experts who use such prototypes and also what the limits are of such tools in CBR-adaptation. When adaptations are guided by experience grained through trial and error by experts, interpolation tools become well-suited methods for automatically and quickly providing adaptation strategies and knowledge through training phases.

Keywords: Case-based reasoning, adaptation, interpolation, artificial neural network, radiation protection, 3D numerical phantoms.

1. Introduction

Case-Based Reasoning (CBR) is a problem solving method that uses similar solutions from similar past problems in order to solve new problems [1]. One of the main properties of the CBR system is its ability to adapt known solutions to find unknown solutions and many adaptation strategies can be

found for this in the literature. Adaptation by generalisation/specialisation requires a hierarchical organisation of the CBR source cases according to generalisation/specialisation relations. Some characteristics are hidden in the generalisation process whereas special ones are added to the general case during the specialisation process.

Adaptation through the use of rules [2] consists of computing the solution of a target case by applying a function to it, using as parameters the solution to a source case that presents some similarities.

Differential adaptation [3] is based on the evaluation of variations found between source and target cases: an approximate solution for the target case is computed by applying the variations between the target case and the source case to the solution of the source case under consideration.

Conservative adaptation [4] is based on *Revision Theory* that considers knowledge modifications. This type of adaptation is based on minimising modifications applied to knowledge. A cost for the possible adaptations must be computed.

Some studies have highlighted the advantages of prototype-based classifications for CBR-systems [5, 6, 7]. These approaches consist of choosing prototypes as representatives for each class of case. Prototypes are also interesting when solutions are not well-known. For example, if you observe someone sitting opposite you, though if it is not possible to model an accurate three-dimensional (3D) representation of his/her lung contours without 3D medical scans, you can nevertheless create a prototype of the organ contours. In such a case, interpolation tools may provide prototypes of an accurate representation of target cases.

Since rules can be discovered only through experience, interpolation tools become the best suited method for adapting solution(s) of source case(s) to target case(s). Furthermore, interpolation tools can be trained to automatically provide the required adaptation knowledge. Indeed, P. Perner and A. Attig in [8, 9] implemented them to evaluate the accuracy and the pertinence of sets of prototypes chosen among a set of known ones. The drawback of such a method is that it is not intelligible to users since the interpolation tool functions like a black box [10]. B. Pandey and R.B. Michra proposed a CBR-based system that uses a programme called Artificial Neural Network (ANN) but only during the retrieval phase [11].

We designed a generic method to use interpolation tools during the adaptation phase of a CBR-based system. This method consists in interpolating new solutions from the know prototypes of the case-base. Its applicability

was also tested and evaluated through implementation in our *CBR designed for Health Science* (CBR-HS) called EquiVox.

In the first part of this paper we present a model of how interpolation tools can be used during the adaptation phase of CBR-based systems. In the second part we present and analyse the example of the EquiVox application in which ANNs were implemented in order to adapt 3D numerical representations of organ contours. The results are then presented and discussed.

2. Method

2.1. Case model and retrieval phase

In CBR approaches, a case is defined as a $\{problem, solution\}$ association. The *problem* part can be represented using a set of n descriptors and the solution by means of a set of N elements. Thus, a source case s and a target case t are defined as follows:
$s = \{pb^s, sol^s\} = \{\{d_i^s\}_{i\in\{1,\dots,n\}}, \{e_i^s\}_{i\in\{1,\dots,N\}}\}$
$t = \{pb^t, sol^t\} = \{\{d_i^t\}_{i\in\{1,\dots,n\}}, \{e_i^t\}_{i\in\{1,\dots,N\}}\}$

The retrieval phase lies in sorting the source cases according to their similarity with the target case. We implemented a classical version of the *k-Nearer Neighbour (kNN)* algorithm [12] which computes the distances between each descriptor of the problem parts of target and source cases.

Thus, for each source case i, a similarity index S_i is computed as follows:

$$S_i = \frac{\sum_{k=1}^{n} \frac{\Delta_k - |d_k^i - d_k^t|}{\Delta_k}}{n} \tag{1}$$

where Δ_k is the difference between the maximum and the minimum known values that the descriptor d_k can take. The S_i value is always between 0 and 1. The greater the similarity of i to t, the closer the S_i value to 1.

2.2. Adaptation phase

B. Knight and F.L. Woon [13] used the interpolation method of D. Shepard [14] to retrieve and adapt a solution to a target case over nominal values. Indeed, they have a limited number of possible solutions and the adapted solution sol^t of $t = \{pb^t, sol^t\}$ minimises
$f(sol^t) = \frac{\sum_{i=1}^{2}(dist_{sol}(sol^t, sol^i)^2 . dist_{pb}(pb^t, pb^i)^{-1})}{\sum i{=}1^2 (dist_{pb}(pb^t, pb^i)^{-1})}$ where $dist_{pb}$ (respectively $dist_{sol}$) is the distance in the problem (respectively solution) space and where cases

$i = 1$ and $i = 2$ are the source cases most similar to t for which $pb^1 \leq pb^t \leq pb^2$.

A. Cordier *et al.* [15] used *Influence functions* that link variations in problem descriptors to those in solution descriptors. They also used *Dependencies* which are relationships between problem and solution descriptors. They indicate whether each problem descriptor impacts each solution element ($Dependency(e_i, d_j) = TRUE$ if e_i depends on d_j, $Dependency(e_i, d_j) = FALSE$ otherwise). In fact, the *Influence function* of e_i takes as parameters the set of d_j for which $Dependency(e_i, d_j) = TRUE$.

Our approach merges these two, considering interpolation tools as *influence functions* of $e_i^t, \forall i \in \{1, ..., N\}$. Thus, we assume $S = \{pb^S, sol^S\}$ is the source case most similar to t, which means $S_S \leq S_i \forall i \in \Omega$ where Ω is the set of all the source cases. For each $e_i, i \in \{1, ..., N\}$, we considered the entire set of problem descriptor items $\Omega_{dep}^i = \cup\{j\}$ for which $Dependency(e_i, d_j) = TRUE$. The interpolation function $Interpolate_i()$ of e_i used as *Influence function* is then given by Equation 2:

$$e_i^t = Interpolate_i(\cup_{j \in \Omega_{dep}^i}\{d_j^t - d_j^S\}, \cup_{j \in \Omega_{dep}^i}\{d_j^S\}, e_i^S) \quad (2)$$

The dependency matrix is furnished by the experts in the domain. Dependency, in fact, may reflect real values. Nevertheless, interpolation tools such as ANNs only need input descriptor values in order to interpolate solution elements. During a preliminary learning phase, these interpolation tools compute, alone, the degree of dependencies between input and output values (ANN synaptic weights, in our case) during a preliminar learning phase. Thus, in our approach, the useful information is whether or not the problem descriptor has any influence on any part of the solution.

3. EquiVox application

In case of accidental exposure to radiation, a dosimetry evaluation must be established for each potential victim (subject) as soon as possible. This evaluation is usually based on available *3D voxel phantoms*, numerical models created from medical images to represent a subject with maximum realism. Examples of voxel phantoms for dosimetric assessment following internal contamination or external exposure are found in the literature [16, 17]. However, existing models are used even if their characteristics differ from the subject's

biometrical data. Dosimetry assessment accuracy and the resulting decontaminating medical action are nevertheless highly dependent on the similarity between phantom and subject.

3D phantoms provide solutions to many situations. In case of accidental exposures, the computed impacts of both the external and internal (inhaled) doses are reported. EquiVox 3D phantoms are used in this particular case, to estimate the dose due to the quantity inhaled. These representations are of precious help for dosimetric reports of inhaled substances since in this particular case, even if the radiation source is not well-known, an accurate idea of the inhaled dose can be computed and accurate representations of organ volumes are required.

Other non-ionizing imaging methods such Magnetic Resonance Imaging and ultrasound may provide accurate images as well. These methods, however, require expensive and highly specialised equipment which may not be readily available after the accident. If it is available anywhere nearby, it may already be in use by local hospitals and accessible only by appointment, which significantly increases delays before any accurate images can be obtained. In addition, radiotherapy services today treat an increasing number of cancerous lung tumours, with physicians and medical doctors using Treatment Planning Systems to treat tumours. The equipment necessary for this requires preparation and control. Its suppliers use 3D phantoms to control their calibration, though it would be reassuring to also use 3D representations from independent sources.

Finally, the use of this equipment requires additional appointments, with further and inconvenient testing, thus creating additional constraints. The already weakened subjects (elderly patients in the case of cancer treatment and patients in shock in the case of accidental exposure) are thus under greater stress and in need of quick reassurance. Consequently, 3D phantoms are useful alternatives and also comprise preliminary models in all cases of exposure to radiation. Hence, the current study aims at assisting the physician in choosing and customising the most similar phantom from among the existing and available ones.

A number of articles on CBR-HS are available [18, 19]. Combinations with *Artificial Intelligence* (AI) tools are also to be found [20, 21, 22]. E.B. Reategui *et al.* [23] combined neural networks with CBR in a diagnostic system for congenital heart diseases. In their approach, the neural network is trained by means of cases stored in the library, and is used during the consultation process to both hypothesise possible diagnostic solutions and to

guide the search for similar cases. EquiVox [24] is a CBR-HS system that also combines an AI tool with a CBR-HS system, but in the adaptation rather than in the retrieving process as in Reategui's approach. Indeed, EquiVox uses the CBR-approach to find the most similar phantom(s) within any set of phantoms and then attempts to adapt them to the characteristics of the target case (the subject) using Artificial Neural Networks (ANNs) [25]. At this point in our investigation, EquiVox can process the 3D contours of three organs: lungs, heart and oesophagus.

A large number of phantoms can be found in the literature [16, 17] where radiation protection is also divided into numerous sub-domains. Indeed, some phantoms are commonly used by experts for external radiotherapy, and others are used by other physicians for evaluation of internal doses received. In fact, experts all have their own collection of 10 to 20 phantoms. When a physician's usual phantoms are all too distant from the subject, the experts must create a new one. Using iterative 3D dilations and contractions, they modify the contours of the 3D organs of their phantoms to make them correspond to those of the subject. They then assemble them to obtain the final phantom on which the computations will be based [16]. In addition, these transformations are only driven by experience, trial and error, and may take many hours or more. The delay also increases with the number of subjects, whereas the problem resolution delay may be limited. In the case of massive irradiation for example, when a disaster such as a nuclear explosion occurs, dosimetric reports are required for hundreds of people of different sizes. In fact, the creation of new organ contours requires a fast data-driven method, and since there is no physical law to govern its design, experts are not able to explicit a rule for the transformation of an organ contour. Thus, the main challenge for EquiVox is to reproduce the same transformation process automatically, without human intervention. Another requirement is that every subject increases the accuracy of dose calculations. Current implementation relies on phantoms that are usually used by a team of experts for pulmonary anthroporadiametry which consists of evaluating the internal dose inhaled [17].

Figure 1 presents the technologies that were used and the data flows over the EquiVox architecture. The whole phantoms are all stored under Rhino3D files. The corresponding biometric data are stored under an ontology scheme (data flow ♯0). The contours of the lungs, heart and oesophagus are extracted (data flow ♯1) and then transmitted to the ANN training module (data flow ♯2), which creates three ANNs (data flow ♯3): one per organ. When a new

phantom is required, the target case description is transmitted to the retrieval module (data flow ♯4) which determines the similitude index by taking into account the source cases (data flow ♯5). If required by the experts, the thorax adaptation module sends the characteristics of the source cases (data flow ♯6) to the ANN interpolation module (data flow ♯7) which loads the trained ANNs (data flow ♯8) and the coordinates of the organ contour in question (data flow ♯9) in order to create interpolated contours suited to the target case (data flow ♯10), which are combined to create the interpolated organ contours (data flow ♯11).

3.1. Case modeling and retrieval phase

When radiation overexposure occurs, the expert's first task is to choose the most accurate 3D phantom according to the subject's height. Indeed, a study by I. Clairand *et al.* [26] demonstrated that the volume and shape of the lungs depend only on the subject's height. In addition, the heart and oesophagus occupy the empty spaces between the lungs. Thus, in EquiVox, the problem part of a case i is described with the subject's height $pb^i = \{h_i\}$. The solution part is a set of 3 3D contours of organs: $sol^i = \{P_i\} = \{P^i_{Lungs}, P^i_{Heart}, P^i_{Oeso.}\}$ where $\forall O \in \{Lungs, Heart, Oeso.\}, P^i_O$ is a set of q_O points joined by a Delauney mesh [27]: $P^i_O = \{C^{i,O}_1, \cdots, C^{i,O}_q\}$ where $C^{i,O}_j$ denotes the 3D coordinates of the point j of the organ O of the case i. Finally, a case i is equal to $\{h_i, \{P^i_{Lungs}, P^i_{Heart}, P^i_{Oeso.}\}\}$. As before, t remains the target case.

The purpose of this phase is to sort the organ contours of the EquiVox case-base according to their similarity to t. As presented in 2.1, a classical algorithm for similarity calculation was used, namely the kNN algorithm. Considering 20 cm $\leq$ human height $\leq$ 250 cm, Equation 1 becomes $S_i = \frac{230-|h_i-h_t|}{230}$.

For example, considering the phantoms stored in EquiVox whose heights are reported in Figure 2, if a Physician has to compute a dosimetric report for someone whose height is 170 cm, P_4 should be retrieved as the most accurate phantom with $S_4 = 0.9914$.

3.2. Adaptation of 3D organ contours

Once a matching case is retrieved, the expert can decide whether or not to use the organ representations of the most similar source cases, or to require the EquiVox platform to generate new ones, adapting the source cases to the

target case. Indeed, assuming SIM is the source case most similar to t, if h_{SIM} and h_t are too different, the expert may decide to adapt SIM or even to create new organ contours which may be re-used for other problems later.

For all the solutions of the source cases, the same number of points defines the 3D contours of the lungs ($q_{Lungs} = 26723$), oesophagus ($q_{oeso.} = 7485$), and heart ($q_{Heart} = 7895$). The points were plotted in the same order and in the same Cartesian coordinate system. Thus, the task of the organ contour-adaptation phase of EquiVox consists of interpolating the 3D coordinates of the points of t in the same order and in the same Cartesian coordinate system. A Delaunay mesh can then be applied so as to create the contours of the organs of t. As concluded by I. Clairand's study [26], organ shapes and volumes of case i depend on h_i:
$Dependency(P_O^i, h_i) = TRUE \ \forall O \in \{Lungs, Heart, Oeso.\}$.

Since the mesh and the number of points are not variable, the adaptation must be carried out on the point coordinates of the organ contours, point by point. Since no formal equation exists, we need a learning method to discover the rules that transform the coordinates of the points of one organ contour into other coordinates. Consequently, data-driven methods using inductive reasoning are the most suitable approaches; ANN and Fuzzy-ANN meet these requirements. We chose ANN as the tool for this step, assuming it might serve as the basis for further work with Fuzzy-ANN if the first results were not convincing. We explored the possibility of using perceptrons with one or two hidden layers trained with a back propagation-based method, but other interpolation tools may also be easily used by EquiVox: the purpose of this study was not to compare interpolation tools, but to provide and validate a general method for using a given interpolation tool.

Each $C_j^{t,O}$ is interpolated from $C_j^{SIM,O}$, h_i and $\Delta h = h_{SIM} - h_t$. Thus, there are 3 ANNs (one for each organ) and Equation 2 becomes $P_O^t = Interpolate_O(\Delta h, h_{SIM}, P_O^{SIM}), O \in \{Lungs, Heart, Oeso.\}$.

For example, in the adaptation of someone with a height of 170 cm, we saw in the previous section that $SIM = 4$ since P_4 was retrieved as the most accurate phantom. Each point of the contour of the lungs of the corresponding phantom representing this subject should then be computed as $P_{Lungs}^{P_{170cm}} = Interpolate_{Lungs}(1.97, 168.03, P_{Lungs}^4)$.

Indeed, the height of P_4 is 168.03 cm and $170 - 168.03 = 1.97$. This subject's lungs are interpolated according to the lungs of the most similar case and the distance between them. Similarly, heart and oesophagus contours are computed by the interpolation tools as follows $P_{Heart}^{P_{170cm}} =$

$Interpolate_{Heart}(1.97, 168.03, P^4_{Heart})$ and
$P^{P_{170cm}}_{Oeso.} = Interpolate_{Oeso.}(1.97, 168.03, P^4_{Oeso.})$.

ANN learning consists of determining the synaptic weights between neurons of different layers and also the optimum number of neurons in hidden layers. First, a random number of neurons per and in the hidden layer(s), along with random values for the synaptic weights are set. The synaptic weights are then computed until the mean distance d_w between the interpolated and the expected phantoms is inferior to a given ε. After optimisation of these synaptic weights, the mean distance d_n between interpolated and expected yet unused phantoms (those in the validation set) is computed. If d_n is superior to a given ε, the number of neurons in hidden layer(s) are changed and the synaptic weights are computed again. This process is performed until $d_n \leq \varepsilon$. Consequently, for this preliminary phase, two sets of elements must be constituted: 1) the elements of the *learning set* with which the optimal synaptic weights are computed and 2) the elements of the *validation set* with which the optimal number of neurons and hidden layers are computed. Naturally, each element can belong to only one of these sets. Generally, 10% of the elements are used for the validation set and 90% for the learning set. Then come the other elements of a *test set* required to verify the ANN accuracy.

In Figure 2, the 12 heights, corresponding to P_1 through P_{12}, are reported on the same axis. Since we have a limited number of 3D Organ Contours (3DOC), we studied the interpolation accuracies regarding the composition of the learning and validation sets. We thus defined two main configurations and four possibilities for each as shown in Table 1. Generally, validation sets are composed of 10% of learning sets. For each possibility the validation set was therefore composed of one phantom: P_3 for $Possibility\sharp 1$, P_4 for $Possibility\sharp 2$, P_7 for $Possibility\sharp 3$ and P_9 for $Possibility\sharp 4$. Cross-validation was then performed for the other sets. We chose four phantoms for the validation sets: one of the smallest (P_3), one slightly smaller than average (P_4), one slightly taller than average (P_7) and one of the tallest (P_9). After having fixed the test and the validation sets, all the remaining phantoms were put into the learning set. For the first configuration the constraint over the ANN input $\Delta h > 0$ was added, whereas for the second $\Delta h < 0$ was required. Then, for each configuration, we explored the possibility of extracting one particular phantom from the learning set to be included it in the validation set.

4. Results

The Equivox platform was implemented and tested on a Personal Computer equipped with an Intel Core i3 CPU, 2.53 GHz, and 4 GiB RAM. Protégé was used to store the descriptor values. Two programming languages were used: Java and C++. All of the programmes were developed by our team. The phantoms were drawn using Rhino3D. The ANN learnings were carried out in C++ at the supercomputer facilities of the Mésocentre de calcul de Franche-Comté, containing 74 nodes based on Intel processors (4 to 6 cores) and 12 to 96 GB of RAM.

The detailed results for each of the three adapted organs are presented below prior to a presention of a global result analysis of the adaptation of 3DOC.

Tables 2 and 3 show the distances obtained between interpolated and expected points for lungs (in $\times 10^{-3}$ cm). Note that it is not possible to interpolate P_1' 3DOCs with constraint ($\Delta h > 0$) or P_{12} with constraint ($\Delta h < 0$). With the constraint $\Delta h > 0$, the learning configuration that gave the most accurate interpolations is the one with $\{P_9\}$ as the validation set. Most of the differences were of approximately 0.02 mm. Accuracies vary from 0.015 mm (interpolation of P_4 with $\{P_9\}$ as the validation set) to 0.642 mm (interpolation of P_5 with $\{P_7\}$ as the validation set). Nevertheless, even in such a case, the adaptation is sufficiently accurate since it is inferior to spatial resolutions of phantoms used by experts ($1.8mm \times 1.8mm \times 4.8mm$). Interpolations with $\Delta h > 0$ are generally better than with $\Delta h < 0$. Contrary to what might be expected, the best adaptations of P_{i+1} and P_{i-1} are not always obtained when $\{P_i\}$ is the validation set. For example, the best interpolations of P_4 and P_2 are obtained when it is P_9 that is in the validation set, not P_3. Similarly, interpolations of P_8 are better with $\{P_4\}$ as the validation set than with $\{P_9\}$ and $\{P_7\}$. Thus, the best interpolations are not obtained when the 3D Lung contours of the phantom having the closest height are included in the validation set.

Globally, the heart interpolations are of greater accuracy than those for the lungs. As shown in Tables 4 and 5, a smaller global deviation may be observed even if there is a great difference for the interpolation of P_5 with $\{P_4\}$ as the validation set (0.646 mm); all the other differences vary from 0.009 mm (interpolation of P_9 with $\{P_7\}$ as the validation set) to 0.098mm (interpolation of P_3 with $\{P_9\}$ as the validation set). Unlike the lung interpolations, the configuration $\Delta h < 0$ provides better interpolations, and,

generally, the configuration with $\{P_3\}$ as the validation set produced the most accurate interpolations. As for the lungs, adaptations are accurate enough since they are inferior to spatial resolutions required by dosimetric reports, and additionally, no correlation is observed between the 3DOC used as the validation set and the best interpolated ones.

As shown in Tables 6 and 7, the oesophagus interpolations were less accurate than those for the previous organs. Specifically, they are roughly only one tenth as accurate as for lungs: from 0.075 mm (interpolation of P_2 using $\{P_4\}$ as the validation set) to 14.3 mm (interpolation of P_5 using $\{P_3\}$ as the validation set). This is the only case for which the requirements of experts are not met. As for the other organs, no correlation can be found between the best interpolations of each 3DOC and the validation set used. All together, the best interpolations for all 3 organs were obtained using $\{P_3\}$ as the validation set.

Finally, one configuration did not always provide the greatest accuracy for all the 3DOCs of one phantom. For example, P_{11}, with $\{P_4\}$ as the validation set and $\Delta h > 0$, produced the best lung adaptations, whereas with $\{P_9\}$ as the validation set and $\Delta h < 0$, it gave the best results for heart contours, while $\{P_3\}$ with $\Delta h < 0$ was most accurate for the oesophagus. Similar results can be observed for all the other phantoms in addition to P_6. Indeed, the organs of P_6 are optimised with the same configuration ($\{P_4\}$ and $\Delta h > 0$).

5. Discussion

Figure 3 shows P_6 interpolated 3DOC and their accuracies using $\{P_4\}$ as the validation set and $\Delta h > 0$. Each point is coloured according to its interpolation error, from blue (the lowest) to red (the highest). We can observe that there is no mesh problem and no artefact is added. In addition, 3D contours show a relatively realistic representation of lungs, heart and oesophagus.

As a general remark, we observe the greatest difficulty in the interpolation of P_5. However, in all but one of the tested cases, the requirements of the experts are satisfied. Indeed, only once are the interpolation deviations superior to the commonly used voxel dimensions used by radiation protection experts. In addition, the same configuration does not always give the best results. These observations and the deviations obtained may be explained

by the fact that all the 3DOCs were designed manually and consequently contain biases.

These results emphasise the importance of the configuration and the 3DOC chosen for each set (validation and training), since the inclusion of one 3DOC in the validation set can generate an accuracy greater than any other and which is sometimes twice as high. Also, the inclusion of one 3DOC in the validation set may introduce a bias for some interpolations while simultaneously improving the accuracy of another target case. These biases may be eased by the capitalisation process: their impact will decrease as the number of source cases rises. Nevertheless, for each adaptation, choosing the training and validation sets with care may provide an additional solution for alleviating the biases introduced by source case solutions.

In addition, the interpolations take only one to three seconds, a great help to physicians who usually need many hours to adapt a single phantom. Thus, extending the use of this method to other organs may result in a useful tool in case of massive accidental radiation exposure.

More generally, we have presented a generic method for the use of interpolation tools in adapting a source-case to a target-case solution within a CBR-system. Its applicability has been confirmed through its implementation in EquiVox, a CBR-HS which responds to the requirements of the specific issue of radiation protection. The results tend to prove that the accuracy of adapted solutions mostly depends on the accuracy of the solutions furnished by the source cases. During its revision process, however (and with user help), a CBR can evaluate the accuracy of adapted solutions. A. Cordier *et al.* [15] proposed that the remarks made by the users during revision processes should be used in the adaptation phase. Future study will focus on how to take revision remarks into account during CBR-adaptation phases driven by interpolation tools.

Finally, examples of adaptation of lungs, oesophagus and heart depend only on one dimension. Other measurements will be required in order to provide adaptations for other organs such as the ribs, the muscles, the skin, the fat, etc. Future investigation will test our approach in practical cases of multidimensional problem descriptions.

6. Conclusion and Perspectives

In this paper our main contribution is the design of a generic method for the use of interpolation tools as influence functions for CBR-adaptation.

The method's applicability has been proved since it was applied in EquiVox, a CBR-HS which can provide prototypes of 3D contours of organs based only on the subjects' height. The resulting accuracies were analysed and discussed with respect to the requirements of the field of application. These results confirm and quantify the general drawback of using interpolation as the means of adaptation in CBR systems [28]: imperfections are introduced into the adapted solutions. Consequently, two improvements are now under consideration. The first consists of collecting and capitalising on phantoms so as to progressively attenuate the imperfections of the solutions; the ANN interpolations, based on ever larger learning sets, will gradually improve. However, a second and more general option must also be explored, which depends on associating vectors to the learning set so as to optimise interpolation accuracies and to determine, a priori, the best learning and validation sets for each target case. Some of the interpolation errors were related to imperfections that may be found in the source-case solutions. Thus, further investigation will need to focus on the elaboration of an adaptation algorithm capable of taking into account the reliability of a source-case solution. Our goal, in other words, is to propose a tool that creates rules for the adaptation of target cases by using confidence indices. This could be attempted through the Genetic Algorithm and/or use of metaheuristics as proposed by Z. Liao *et al.* [29].

7. Acknowledgements

The authors wish to thank the *Institut National de la Santé et de la Recherche Médicale*, the *Ligue Contre le Cancer*, the *Pays de Montbéliard Agglomération* and the *Société Française de Radioprotection* for their financial aid, the *National Institute of Radiological Protection and Nuclear Safety* for their expertise, and John Olsen for his help with the English language.

References

[1] Kolodner, J.: Case-based reasoning. San Mateo, CA: Morgan Kaufmann (1993)

[2] Melis, E., Lieber, J., Napoli, A.: Reformulation in Case-Based Reasoning. In:Forth European Workshop on Case-Based Reasoning, Lecture Notes in Artificial Intelligence, Springer, 1488:172–183 (1998)

[3] Fuchs, B., Lieber, J., Mille, A., Napoli, A.: A general strategy for adaptation in Case-Based Reasoning. In: LIRIS Report RR-LIRIS-2006-016, http://liris.cnrs.fr/publis/?id=2477 (2006)

[4] Lieber, J.: Application of the Revision Theory to Adaptation in Case-Based Reasoning: the Conservative Adaptation. In: Proceedings of the 7th International Conference on Case-Based Reasoning, Lecture Notes in Artificial Intelligence, Springer, 4626:239–253 (2007)

[5] Bichindaritz, I., Marling, C.: Case-based reasoning in the health sciences: Whats next? In: Artificial Intelligence in Medicine 36: 127-135 (2006)

[6] Bichindaritz, I.: Prototypical Cases for Knowledge Maintenance in Biomedical CBR. In: Proceedings of International Conference on Case-Based Reasoning, Belfast, 492–506 (2007)

[7] Little, S., Colatino, S., Salvetti, O., Perner, P.: Can Prototype-Based Classifica-tion be a good Method for Biomedical Applications? In: Trans. MLDM (MLDM) 2(1): 44–61 (2009)

[8] Perner, P., Attig, A.: Using Prototype-Based Classification for Automatic Knowledge Acquisition. In: Patrick Shen-Pei Wang (Ed.), Pattern Recognition, Machine Intelligence and Biometrics, Springer Verlag: 197–212 (2011)

[9] Attig, A., Perner, P.: Incremental Learning of Model for Watershed-Based Image Segmentation. In: R.P. Barneva et al. (Eds): IWCIA 2012, LNCS 7655, Springer-Verlag: 209–222 (2012)

[10] DAquin, M., Lieber, J., Napoli, A.: Adaptation Knowledge Acquisition: A Case Study for Case-Based Decision Support in Oncology. In: Computational Intelligence, 161–176 (2006)

[11] Babita Pandey, Michra, R.B.: An integrated intelligent computing model for the interpolation of EMG based neuromuscular disease. In: Expert Systems With Applications 36, pp. 9201-9213 (2009)

[12] Cover, T., Hart, P.: Nearer Neighbour Pattern Classification. In: IEEE Transactions on Information Theory 13:21–27 (1967)

[13] Knight, B., Woon, F.L.: Case Based Adaptation Using Interpolation over Nominal Values. In: Research and development in Intelligent Systems, Springer, 21:73–86 (2005)

[14] Shepard, D.: A Two-Dimensional interpolation Function for irregularity Spaced Data. In: Proceedings of the 23rd National Conference, ACM, 517–523 (1968)

[15] Cordier, A., Fuchs, B., Mille, A.: Engineering and learning of adaptation knowledge and Case-Based Reasoning. In: Proceedings of the 15th International Conference on Knowledge Engineering and Knowledge Management - EAKW 2006, Springer-Verlag, 303–317 (2006)

[16] Farah, J. and Broggio, D. and Franck, D.: Examples of Mesh and NURBS modelling for in vivo lung counting studies. In: Radiation Protection Dosimetry, NTP, 144(1-4):344–348 (2011)

[17] Broggio, D., Beurrier, J., Bremaud, M., Desbrée, A., Farah, J., Huet, C., Franck, D.: Construction of an extended library of adult male 3D models: rationale and results. in: Phys. Med. Biol. 56: 76597692 (2011)

[18] Bichindaritz, I.: Case-based reasoning in the health sciences: Why it matters for the health sciences and for CBR. In: Althof, K.-D.; Bergmann, R.; Minor, M.; and Hanft, A., eds., Advances in Case-Based Reasoning: 9th European Conference, ECCBR, 1-17. Berlin: Springer (2008)

[19] Bichindaritz, I.: Advances in case-based reasoning in the health sciences. In: Artificial Intelligence in Medicine 51: 75-79 (2011)

[20] Diaz, F., Fdze-Riverola, F., Corchado, J.M.: Gene-CBR: A Case-Based Reason-ing Tool for Cancer Diagnosis using Microarray Datasets. In: Computational Intelligence, 254–258 (2006)

[21] El Balaa, Z., Strauss, A., Uziel, P., Maximini, K., Traphoner, R.: FM-Ultranet: A Decision Support System Using Case-Based Reasoning Applyied to Ultrasono-graphy. In: McGinty, L. (ed.): Workshop Proceedings of the Fifth International Conference on Case-Based Reasoning, NTNU, Trondheim, Norway, 37–44 (2003)

[22] Monati, S.: Case-Based Reasoning for Managing Non-Compliance with Clinical Guidelines. In: Wilson, D.C., Khemani, D. (ed.): Proceedings of Case-Based Reasoning in Health Science Workshop, ICCBR, Belfast, 325–336 (2007)

[23] Reategui, E.B., Campbell, J.A., Leaob, B.F.: Combining a neural network with case-based reasoning in a diagnostic system. In: Artificial Intelligence in Medicine 9:5–27 (1997)

[24] Henriet, J., Leni, P.E., Laurent, R., Roxin, A., Chebel-Morello, B., Salomon, M., Farah, J., Broggio, D., Franck, D., Makovicka, L.: Adapting numerical representations of lung contours using Case-Based Reasoning and Artificial Neural Networks. In: B. Daz Agudo and I. Watson (Eds.): ICCBR 2012, Artificial Intelligence series, Springer, Heidelberg, LNCS 7466, pp. 137-151 (2012)

[25] McCulloch, W.S. and Pitts, W.: A logical calculus of the ideas immanent in nervous activity. In: Bulletin of mathematical biology, Springer, 5(4):115–133 (1943)

[26] Clairand, I. and Bouchet, L.G. and Ricard, M. and Durigon, M. and Di Paola, M. and Aubert, B.: Improvement of internal dose calculations using mathematical models of different adult heights. In: Physics in medicine and biology, IOP Publishing, 45:2771–2785 (2000)

[27] Christensen, G.E.: Deformable shape models for anatomy. Thesis, Washington University (1994)

[28] Chatterjee, N. and Campbell, J.A.: Interpolation as a means of fast adaptation in case-based problem solving. In: Proceedings Fifth German Workshop on Case-Based Reasoning 65–74 (1997)

[29] Zhenliang Liao, Xuewei Maoa, Phillip M. Hannam, Tingting Zhao: Adaptation methodology of CBR for environmental emergency preparedness system based on an Improved Genetic Algorithm. In: Expert Systems With Applications 39:7029-7040 (2012)

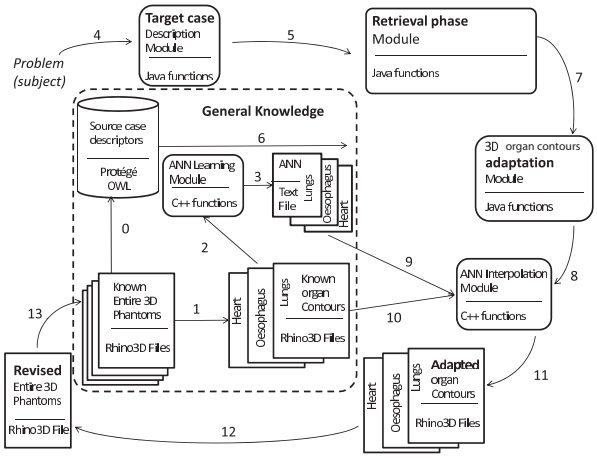

Figure 1: Data flows over the EquiVox architecture.

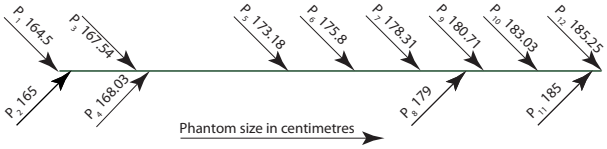

Figure 2: Phantom heights of the available 3D organ contours.

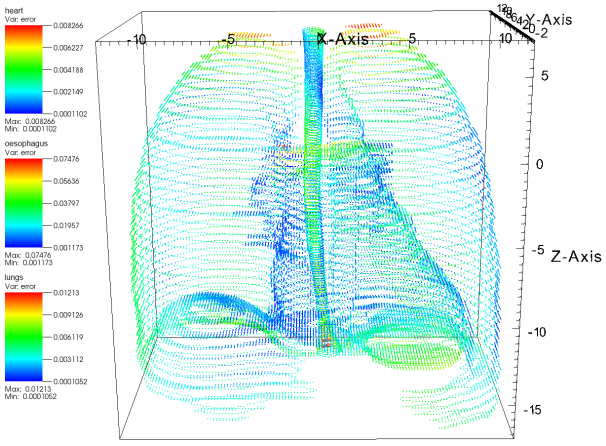

Figure 3: Representation of P_6 interpolated organs with $\{P_4\}$ as the validation set and $\Delta h > 0$.

	Test set	Validation set	Learning set
Possibility ♯1	$\{P_i\}, i \in \{1..12\} i \neq 3$	$\{P_3\}$	$\bigcup_{j\in\{1..12\},j\neq 3,j\neq i}\{P_j\}$
Possibility ♯2	$\{P_i\}, i \in \{1..12\} i \neq 4$	$\{P_4\}$	$\bigcup_{j\in\{1..12\},j\neq 4,j\neq i}\{P_j\}$
Possibility ♯3	$\{P_i\}, i \in \{1..12\} i \neq 7$	$\{P_7\}$	$\bigcup_{j\in\{1..12\},j\neq 7,j\neq i}\{P_j\}$
Possibility ♯4	$\{P_i\}, i \in \{1..12\} i \neq 9$	$\{P_9\}$	$\bigcup_{j\in\{1..12\},j\neq 9,j\neq i}\{P_j\}$

Table 1: Learning, validation and test sets tested.

Val.		Tested 3DOC					
set	Δh	P_1	P_2	P_3	P_4	P_5	P_6
P_3	> 0	/	3.5	/	8.7	23.9	6.7
P_3	< 0	2.6	4.1	/	13.4	4.3	6.9
P_4	> 0	/	6.2	42.9	/	38.7	3.5
P_4	< 0	1.7	2.8	3.7	/	4.5	6.4
P_7	> 0	/	4.2	16.4	3.3	64.2	6.3
P_7	< 0	5.7	2.8	2.7	45.5	3.4	7.4
P_9	> 0	/	2.4	3.4	1.5	12.0	6.8
P_9	< 0	3.6	7.9	3.2	4.4	6.6	5.7

Table 2: Distances ($\times 10^{-3}$ cm) between interpolated and expected points of lung contours of P_1 to P_6.

Val.		Tested 3DOC					
set	Δh	P_7	P_8	P_9	P_{10}	P_{11}	P_{12}
P_3	> 0	2.7	4.1	17.5	25.5	3.7	8.9
P_3	< 0	7.9	8.9	24.9	20.2	7.5	/
P_4	> 0	2.1	2.0	1.9	31.7	1.9	8.5
P_4	< 0	6.2	6.2	4.3	11.8	7.5	/
P_7	> 0	/	7.4	2.2	4.9	2.9	2.3
P_7	< 0	/	8.9	5.0	15.4	4.9	/
P_9	> 0	2.9	6.2	/	8.3	3.3	4.4
P_9	< 0	11.1	4.1	/	9.1	7.3	/

Table 3: Distances ($\times 10^{-3}$ cm) between interpolated and expected points of lung contours of P_7 to P_{12}.

Val.		Tested 3DOC					
set	Δh	P_1	P_2	P_3	P_4	P_5	P_6
P_3	> 0	/	3.1	/	4.9	11.1	4.2
P_3	< 0	2.5	2.3	/	4.9	2.4	4.1
P_4	> 0	/	3.5	24.0	/	64.6	2.3
P_4	< 0	1.2	2.6	2.4	/	6.1	4.6
P_7	> 0	/	2.4	8.6	9.7	18.7	4.5
P_7	< 0	1.4	8.2	0.9	6.6	1.5	4.3
P_9	> 0	/	1.2	9.8	1.2	15.3	4.0
P_9	< 0	1.1	1.3	2.5	2.4	3.9	2.8

Table 4: Distances ($\times 10^{-3}$ cm) between interpolated and expected points of heart contours of P_1 to P_6.

Val.		Tested 3DOC					
set	Δh	P_7	P_8	P_9	P_{10}	P_{11}	P_{12}
P_3	> 0	1.3	7.6	15.3	13.2	2.2	3.7
P_3	< 0	4.3	5.4	2.4	4.6	3.6	/
P_4	> 0	1.9	2.1	1.6	1.9	2.3	3.9
P_4	< 0	3.5	11.5	2.0	3.3	1.3	/
P_7	> 0	/	3.9	0.9	2.9	2.4	1.5
P_7	< 0	/	2.3	11.4	1.9	1.2	/
P_9	> 0	1.3	4.3	/	5.7	1.8	1.8
P_9	< 0	5.5	0.8	/	26.0	1.1	/

Table 5: Distances ($\times 10^{-3}$ cm) between interpolated and expected points of heart contours of P_7 to P_{12}.

Val.		Tested 3DOC					
set	Δh	P_1	P_2	P_3	P_4	P_5	P_6
P_3	> 0	/	19.6	/	20.5	1426.6	35.9
P_3	< 0	10.3	32.3	/	74.7	26.7	42.7
P_4	> 0	/	7.5	71.3	/	48.8	24.5
P_4	< 0	17.8	53.4	16.7	/	32.5	35.7
P_7	> 0	/	47.4	72.5	17.1	928.9	57.6
P_7	< 0	109.1	130.4	66.5	219.3	112.2	110.8
P_9	> 0	/	26.1	40.9	26.0	130.3	47.0
P_9	< 0	23.9	93.5	19.6	1047.6	41.3	38.0

Table 6: Distances ($\times 10^{-3}$ cm) between interpolated and expected points of oesophagus contours of P_1 to P_6.

Val.		Tested 3DOC					
set	Δh	P_7	P_8	P_9	P_{10}	P_{11}	P_{12}
P_3	> 0	12.4	102.9	25.0	113.9	36.9	17.9
P_3	< 0	109.6	17.9	121.9	49.1	12.7	/
P_4	> 0	29.0	95.4	18.5	162.8	62.6	33.4
P_4	< 0	104.0	10.3	110.5	38.7	23.2	/
P_7	> 0	/	86.1	103.6	108.0	41.8	134.6
P_7	< 0	/	77.7	205.9	105.2	72.4	/
P_9	> 0	29.8	88.8	/	102.5	31.0	32.7
P_9	< 0 38.0	78.5	27.6	/	47.7	37.6	/

Table 7: Distances ($\times 10^{-3}$ cm) between interpolated and expected points of oesophagus contours of P_7 to P_{12}.